AMERICAN SOCIETY FOR MICROBIOLOGY | Applied and Environmental Microbiology®

GENETICS AND MOLECULAR BIOLOGY

Biosynthesis of Aurodox, a Type III Secretion System Inhibitor from *Streptomyces goldiniensis*

Rebecca E. McHugh,[a,b] John T. Munnoch,[a] Robyn E. Braes,[a] Iain J. W. McKean,[a,c] Josephine Giard,[a] Andrea Taladriz-Sender,[c] Frederik Peschke,[c] Glenn A. Burley,[c] Andrew J. Roe,[b] Paul A. Hoskisson[a]

[a]Strathclyde Institute of Pharmacy and Biomedical Sciences, University of Strathclyde, Glasgow, UK
[b]Institute of Infection, Immunity and Inflammation, University of Glasgow, Glasgow, UK
[c]Department of Pure and Applied Chemistry, University of Strathclyde, Glasgow, UK

ABSTRACT The global increase in antimicrobial-resistant infections means that there is a need to develop new antimicrobial molecules and strategies to combat the issue. Aurodox is a linear polyketide natural product that is produced by *Streptomyces goldiniensis*, yet little is known about aurodox biosynthesis or the nature of the biosynthetic gene cluster (BGC) that encodes its production. To gain a deeper understanding of aurodox biosynthesis by *S. goldiniensis*, the whole genome of the organism was sequenced, revealing the presence of an 87 kb hybrid polyketide synthase/non-ribosomal peptide synthetase (PKS/NRPS) BGC. The aurodox BGC shares significant homology with the kirromycin BGC from *S. collinus* Tü 365. However, the genetic organization of the BGC differs significantly. The candidate aurodox gene cluster was cloned and expressed in a heterologous host to demonstrate that it was responsible for aurodox biosynthesis and disruption of the primary PKS gene (*aurAI*) abolished aurodox production. These data supported a model whereby the initial core biosynthetic reactions involved in aurodox biosynthesis followed that of kirromycin. Cloning *aurM** from *S. goldiniensis* and expressing this in the kirromycin producer *S. collinus* Tü 365 enabled methylation of the pyridone group, suggesting this is the last step in biosynthesis. This methylation step is also sufficient to confer the unique type III secretion system inhibitory properties to aurodox.

IMPORTANCE Enterohemorrhagic *Escherichia coli* (EHEC) is a significant global pathogen for which traditional antibiotic treatment is not recommended. Aurodox inhibits the ability of EHEC to establish infection in the host gut through the specific targeting of the type III secretion system while circumventing the induction of toxin production associated with traditional antibiotics. These properties suggest aurodox could be a promising anti-virulence compound for EHEC, which merits further investigation. Here, we characterized the aurodox biosynthetic gene cluster from *Streptomyces goldiniensis* and established the key enzymatic steps of aurodox biosynthesis that give rise to the unique anti-virulence activity. These data provide the basis for future chemical and genetic approaches to produce aurodox derivatives with increased efficacy and the potential to engineer novel elfamycins.

KEYWORDS *Streptomyces*, antibiotic, elfamycin, EHEC, polyketide, aurodox, biosynthesis, kirromycin

Streptomyces bacteria are renowned for their ability to produce a plethora of natural products that exhibit a wide range of chemical structures, activities, and modes of action (1). One such molecule is aurodox, which has a remarkable anti-virulence mode of action in addition to its well-understood anti-Gram-positive properties (2–4). Aurodox is produced by *Streptomyces goldiniensis* and belongs to the elfamycin group of antibiotics, which are characterized by their mode of action rather than their chemical structure (4). The anti-bacterial mode of action of the elfamycins is well understood,

Editor Arpita Bose, Washington University in St. Louis

Address correspondence to Paul A. Hoskisson, paul.hoskisson@strath.ac.uk.

The authors declare no conflict of interest.

Received 21 April 2022
Accepted 26 June 2022
Published 18 July 2022

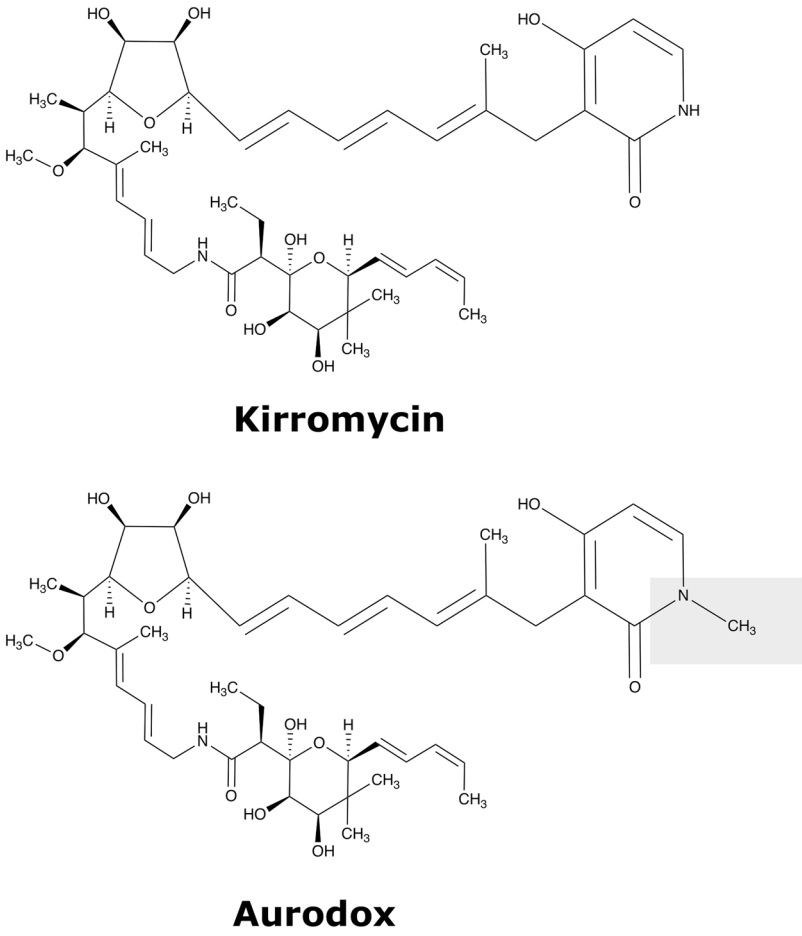

FIG 1 Chemical structures of the elfamycins kirromycin and aurodox. The shaded box highlights the additional methylation site of aurodox located on the pyridone ring.

where they target protein translation through inhibition of elongation factor thermounstable (EF-Tu; (4). Direct EF-Tu binding by kirromycin/aurodox-type elfamycins prevents EF-Tu:GDP from dissociating from the ribosome, preventing elongation and inhibiting protein synthesis (4). Aurodox also has an additional mode of action, originally discovered during a screen for type III secretion system (T3SS) inhibitors in Enteropathogenic *Escherichia coli* (EPEC; (5)). More recently, it was demonstrated that aurodox inhibits T3SS and virulence in enterohemorrhagic *E. coli* (EHEC) and EPEC through an EF-Tu-independent mechanism, involving the downregulation of transcription of the master virulence regulator, Ler (6).

Aurodox was discovered in 1973 (2). It is a linear polyketide compound that is highly similar to kirromycin (7) differing only in methylation of the pyridone moiety. Kirromycin biosynthesis has been characterized and the BGC encodes five large polyketide synthase (PKS) units, which act to form the polyketide backbone, before tailoring enzymes decorate the molecule (7–10). Given the similarity of the molecules, we hypothesized that the aurodox biosynthetic gene cluster (BGC) may be homologous to the hybrid PKS/nonribosomal peptide synthetase (NRPS) BGC of kirromycin, with the addition of an ORF responsible for pyridone-associated methylation (Fig. 1).

In EHEC infections, antibiotic treatment is not recommended due to the prevalence of systemic side effects (11, 12), and the upregulation of the bacterial SOS response in EHEC, resulting in Shiga toxin expression (13–16). The consequences of this are severe for patients with increased Shiga toxin levels being associated with systemic infections and nephrotoxicity (12). Therefore, inhibiting virulence in a specific and targeted

manner, which does not induce Shiga toxin production, represents a promising strategy for repurposing aurodox as an anti-virulence treatment (6).

Here, we presented the identification and cloning of the aurodox BGC followed by confirmation of the genes responsible for aurodox biosynthesis through heterologous expression and gene disruption. The aurodox biosynthetic cluster was found to differ in organization from that of kirromycin. However, based on homology, we proposed a biosynthetic scheme for aurodox. Additionally, we demonstrated through heterologous expression of the putative methyltransferase (*aurM**) that methylation of the pyridone moiety is the last step in aurodox biosynthesis. This improved understanding of aurodox biosynthesis will enable greater exploitation and engineering of aurodox as an anti-virulence therapy and extends our knowledge of an important group of antimicrobial compounds.

RESULTS

Whole-genome sequencing of *S. goldiniensis* revealed a putative aurodox BGC with homology to the kirromycin BGC. To identify the aurodox BGC, the whole genome of *S. goldiniensis* ATCC 21386 was sequenced using a hybrid approach where Illumina, PacBio, and Oxford Nanopore technologies were used to generate a high-quality draft genome (PRJNA602141; (17)). Analysis of the sequence using antiSMASH (18) identified 36 putative BGCs within the *S. goldiniensis* genome (see Table S1 at https://doi.org/10.6084/m9.figshare.19140005.v1; (17)). A large region of the *S. goldiniensis* genome was identified (position 4,213,370 to 4,484,508; 271 kb) that was rich in BGCs, including an 87 kb region with homology to the kirromycin BGC (7). This 87 kb region consisted of 25 open reading frames (ORFs) with 23 ORFs exhibiting >60% similarity to homologs in kirromycin BGC from *S. collinus* (Table 1; see Table S2 at https://doi.org/10.6084/m9.figshare.19140005.v1). Despite the homologous ORFs within the BGCs, clear differences were apparent between the kirromycin and aurodox gene clusters, such as the inversion of NRPS/PKS genes and rearrangements of genes that encode the decorating enzymes of the polyketide backbone (Fig. 2). Two additional genes were identified in the aurodox BGC that lacked homologs in kirromycin cluster (Table 1). A gene encoding a SAM-dependent *O*-methyltransferase (*aurM**), which we proposed catalyzes the addition of the methyl group to the pyridone moiety and a hypothetical protein with no predicted homology to genes of known function (*aurQ*). Given the homology to the kirromycin BGC, it was hypothesized that this putative BGC was responsible for aurodox production in *S. goldiniensis* (Table 1).

Heterologous expression of the putative aurodox BGC in *Streptomyces coelicolor* M1152 resulted in aurodox biosynthesis. To determine if the putative aurodox BGC was responsible for aurodox biosynthesis, a phage artificial chromosome (PAC) library was constructed from *S. goldiniensis* genomic DNA, and the resulting pESAC-13A vectors (19) were screened for the presence of the putative aurodox cluster via PCR (Bio S & T, Canada; Fig. S1 at https://doi.org/10.6084/m9.figshare.19140005.v1; oligonucleotide primers are in Table S5). Two PCR-positive PAC clones were identified that contained the entire region of interest. PFGE was used to confirm the size of the inset and one clone (pAur1) was taken forward for further study (Fig. S1 to S3). The complete PAC was sequenced to identify the boundaries of the pAur1, which contained a 129Kbp insert (see Fig. S2 at https://doi.org/10.6084/m9.figshare.19140005.v1 for pAur1) and the complete region proposed to encode the aurodox BGC.

The introduction of pAur1, which integrates at the ΦC31 integration site, to the *S. coelicolor* M1152 'superhost' was achieved via conjugation from the nonmethylating ET12567/pR9604 strain to avoid the methyl-specific restriction system (20). Importantly, *S. coelicolor* M1152 encodes three copies of EF-Tu, including one copy of the elfamycin-resistant type EF-Tu, *tuf2* suggesting this strain would be a suitable host for expression of aurodox. Exconjugants containing the putative aurodox BGC (pAur1) and empty vector controls (pESAC-13A) were screened via PCR (see Fig. S3 at https://doi.org/10.6084/m9.figshare.19140005.v1) and the resulting strains were cultured in liquid media. Culture supernatant extracts were then subjected to Liquid Chromatography-Mass Spectrometry

TABLE 1 Comparison of aurodox and kirromycin BGC and their functions[a]

Gene	Kirromycin BGC homolog	% homology of aurodox gene with its kirromycin homolog	Function
aurQ	**NA**	**-**	**Hypothetical protein**
aurHV	*kirHV*	98%	Hypothetical protein
aurHI	*kirHI*	97%	Hypothetical protein
aurB	*kirB*	98%	Non-ribosomal peptide synthetase
*aurM**	NA	-	Type I SAM-dependent methyltransferase
aurCI	*kirCI*	97%	S-malonyltransferase
aurOII	*kirOII*	100%	Cytochrome P450 hydroxylase
aurD	*kirD*	97%	Aspartate 1-decarboxylase
aurM	*kirM*	99%	Class I SAM-dependent *O*-methyltransferase
aurCII	*kirCII*	96%	Ethylmalonyl-transferase
aurX	*kirHII*	98%	Dieckmann cyclase
aurHIII	*kirHIII*	95%	DUF6084 domain-containing protein
aurT	*kirTI/TII*	65%	Major facilitator superfamily transporter
aurN	*kirN*	97%	Crotonyl-CoA carboxylase/reductase
AurHVI	*KirHVI*	95%	Hypothetical protein
aurHIV	*kirHIV*	92%	Magnesium ATP-ase
aurAI	*kirAI*	100%	Type 1 polyketide synthase
aurAII	*kirAII*	94%	Trans-AT PKS
aurAIII	*kirAIII*	99%	Non-ribosomal peptide synthetase
aurAIV	*kirAIV*	99%	Trans-AT PKS
aurAV	*kirAV*	99%	SDR family NAD(P)-dependent oxidoreductase
aurAVI	*kirAVI*	94%	Type I PKS
aurR	*kirRI/RII*	56%	TetR/AcrR family transcriptional regulator
aurQ	NA	-	Hypothetical protein
aurHV	*kirHV*	98%	Hypothetical protein
aurHI	*kirHI*	97%	Hypothetical protein

[a]Genes found only in the aurodox cluster are in bold. To be consistent with kirromycin biosynthesis we have maintained the nomenclature between this putative aurodox gene and their kirromycin homologs. NA, not applicable; -, indicates no homologous gene in the kirromycin BGC.

(LC-MS) analysis and compared to an authentic aurodox standard (Fig. 3A). An equivalent aurodox peak was also observed in the trace from *S. goldiniensis* extract (Fig. 3B). Extracts from the *S. coelicolor* M1152/pESAC-13A, empty vector control lacked the distinct peak of aurodox (Fig. 3C), whereas *S. coelicolor* M1152/pAur1, the strain containing the putative aurodox cluster, exhibited the characteristic peak (Fig. 3D). Mass spectrometric analysis revealed peaks at *m/z* 793, corresponding to the molecular ion of aurodox from cultures of *S. coelicolor* M1152/pAur1 and *S. goldiniensis*. This peak was absent from the empty vector control strain (Fig. 3C), indicating that the putative aurodox BGC encodes aurodox biosynthesis in *S. goldiniensis*.

To unequivocally confirm the role of the putative aurodox BGC genes encoded on the pAur1 clone, deletion of the type IPKS (*aurAI*) was performed using ReDirect (21), resulting in pAur1Δ*aurAI*. We hypothesized that the deletion of the primary PKS would prevent aurodox biosynthesis and confirmed the putative BGC was required for aurodox biosynthesis. Analysis of extracts from *S. coelicolor* M1152/pAur1Δ*aurAI* lacked a peak at the aurodox-associated retention time (Fig. 3E) confirming the role of these genes in aurodox biosynthesis.

Bioassays of these culture supernatants using *Staphylococcus aureus* (ATCC 43300) as

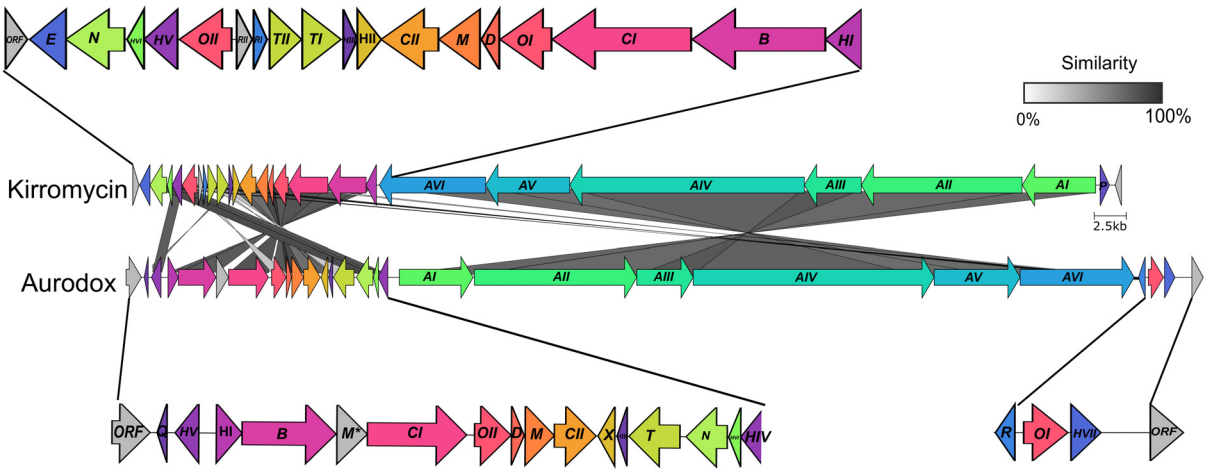

FIG 2 Comparison of aurodox and kirromycin gene clusters. Adjoining lines represent amino acid similarity according to scale. Gray genes represent nonhomologous genes, and * represents the SAM-dependent *O*-methyltransferase AurM*. Figure generated by clinker.py using GCA_018728545.1.

an indicator organism, further support the LCMS data, with *S. coelicolor* M1152/pAur1 inhibiting *S. aureus* growth, whereas the empty vector control (*S. coelicolor* M1152/pESAC-13A) and the deletion strain (*S. coelicolor* M1152/pAur1Δ*aurAI*) display reduced bioactivity (Fig. 3F). The presence of a peak at 6 min in the LC trace from *S. coelicolor* M1152/pAur1Δ*aurAI* could be either a truncated derivative of aurodox produced from the BGC following the mutation of *aurAI* or more likely the activation of a silent BGC elsewhere in the genome, which is responsible for the bioactivity observed against *S. aureus*.

Proposed biosynthesis of aurodox followed that of kirromycin. The ClusterTools algorithm from antiSMASH was used to annotate the core PKS/NRPS genes of the aurodox BGC, including specific module assignments (18, 22). This facilitated the prediction that the catalytic domains of AurI to AurVI largely follow those of KirI to KirVI of the kirromycin gene cluster despite the rearrangements in the overall cluster architecture (Fig. 2 and 4; (7, 9)). In AurAI and AurAII, acetyl Co-A extension is via Claisen condensation reactions (8). However, the PKSs are atypical in arrangement, with two additional dehydratase domains present. While these were not previously identified in the kirromycin pathway (7), reanalysis of the kirromycin pathway using ClusterTools (22) does predict the presence of these domains in KirI to KirVI. Remarkably, no homolog of *kirP*, the kirromycin phosphopantheteinyl transferase (PPTase) was identified in the aurodox BGC.

It is predicted that *aurAIII* encodes a hybrid NRPS/PKS enzyme consisting of consecutive condensation and adenylation domains that catalyze the condensation of glycine and the incorporation of the amide bond, a process conserved with the kirromycin pathway. The enzymes AurAIV-AVII are predicted to extend the aurodox backbone before AurB (which possesses the conserved DTLQLGVIWK motif (23), catalyzes the incorporation β-alanine, presumably synthesized by the putative aspartate-1-decarboxylase, AurD (Fig. 4 and Table 1).

A SAM-dependent methyltransferase, *aurM, catalyzed the conversion of kirromycin to aurodox.** An additional SAM-dependent methyltransferase (AurM*) was identified in the aurodox BGC, which was absent in the kirromycin BGC. It was hypothesized that AurM* catalyzes the conversion of kirromycin to aurodox and may be the last step in aurodox biosynthesis. To test this, *aurM** from *S. goldiniensis* was cloned into an integrating vector (pIJ6902; (24)) and introduced into *Streptomyces collinus* Tü 365, a natural kirromycin producer. Empty vector controls of *S. collinus* Tü 365 containing pIJ6902 showed no species corresponding to aurodox but did show the presence of kirromycin compared to an authentic standard (Fig. 5A and 5B). LCMS analysis of solvent extracts from *S. collinus* Tü 365 expressing *aurM** revealed characteristic peaks corresponding to aurodox and kirromycin (Fig. 5C), with negative scan MS showing an *m/z* ratio of

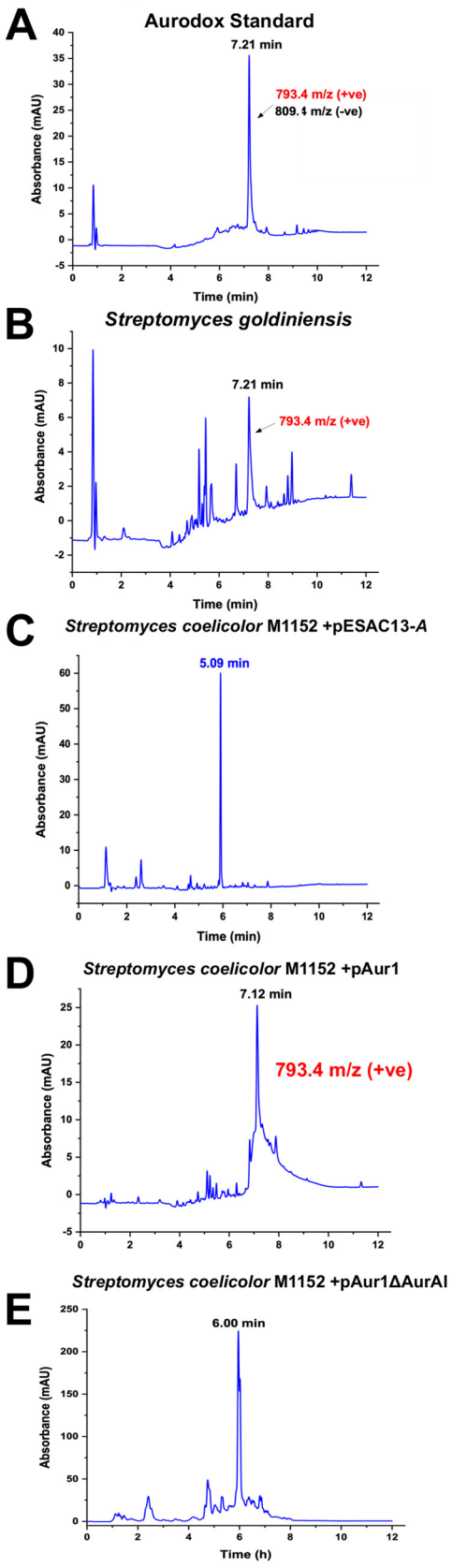

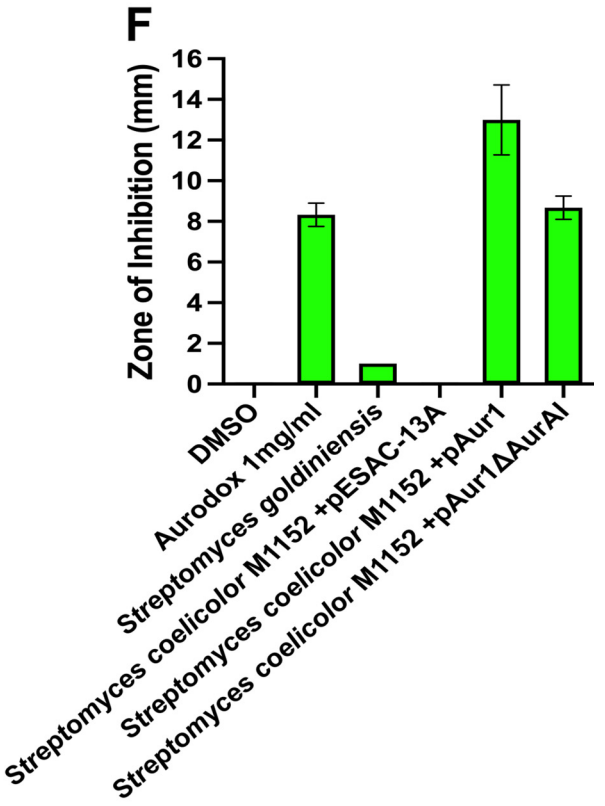

FIG 3 Heterologous expression of aurodox biosynthesis in *Streptomyces coelicolor* M1152. Chromatograms of aurodox standard (Enzo; A). The peak at aurodox retention time is indicated. (B) Chromatogram from wild-type *Streptomyces goldiniensis* indicating aurodox production.

(Continued on next page)

793, corresponding to aurodox in addition to an *m/z* ratio 795 which corresponds to kirromycin (Fig. 5A). This indicates that AurM* is responsible for the methylation of kirromycin as a precursor to aurodox formation.

DISCUSSION

Understanding the mode of action, resistance mechanisms and the biosynthesis of useful natural products is key to their development for clinical application. The linear polyketide, aurodox, while being known for almost 50 years, was recently found to exhibit novel anti-virulence activity via a previously unknown target (6), yet nothing was known about its biosynthesis. While aurodox is structurally similar to kirromycin, it is now well known that structurally identical or highly similar natural products can be biosynthesized via diverse chemical routes (1, 25–28), suggesting that there is still much to be learned from studying the biosynthesis of structurally similar natural products in terms of novel activity and evolution of natural products.

Despite similarities in structure, anti-bacterial mode of action, and core BGC machinery between aurodox and kirromycin, key differences in biosynthesis were identified. The aurodox cluster is ~80% similar to the kirromycin BGC, sharing 23 of the 25 genes, with seven genes within both clusters encoding hypothetical proteins with no assigned function. There is no apparent PPTase (*kirP* homolog) encoded in the aurodox cluster, which would normally posttranslationally modify the acyl carrier protein (ACP) to facilitate the extension of the PK/NRP chains during assembly, suggesting that this function may be fulfilled by a promiscuous PPTase encoded elsewhere in the genome (29). Remarkably, no thioesterase domain was identified in the PKS-NRPS megasynthases. There is a putative Dieckmann-like cyclase encoded within the cluster (*aurB*), which may be responsible for the cleavage and cyclization of the aurodox molecule, a mechanism that has recently been proposed in a few other pyridone natural products (30). The anti-virulence activity of aurodox requires methylation of the pyridone ring, which is catalyzed by *aurM**. The 'magic methyl' effect is well known in drug discovery for enhancing the activity and pharmacological properties of drugs (31, 32), and the kirromycin to aurodox transformation indicates that this has been exploited in nature to alter the activity of natural products. Moreover, this indicates that the derivatization of the pyridone ring of kirromycin may be a useful strategy for diversifying elfamycin activities. Regarding the origin of *aurM**, two additional *O*-methyl transferases are encoded within the *S. goldiniensis* genome, each with ~35% amino acid similarly to AurM*, which may suggest that *aurM** was acquired by horizontal gene transfer (HGT) rather than duplication of an existing *O*-methyltransferase from the genome of *S. goldiniensis*, and offers insight into the evolution of novel activities in natural products and the potential of this to be driven through HGT of single ORFs.

Overall, this greater understanding of the biosynthesis of aurodox and the steps that contribute to unique modes of action will enable us to explore the potential of aurodox as a therapeutic agent for EHEC treatment in the food chain and the clinic

MATERIALS AND METHODS

Growth and maintenance of bacterial strains. The bacterial strains used in this study are detailed in Table S3 at https://doi.org/10.6084/m9.figshare.19140005.v1. Genetic constructs used and their antibiotic selection is described in Table S4. Routine growth and maintenance procedures were carried out according to Kieser et al. (33). A list of oligonucleotides used in this study can be found in Table S5.

Whole-genome sequencing of *Streptomyces goldiniensis*. Genomic DNA was extracted from *S. goldiniensis* using the Streptomyces DNA isolation protocol described by Kieser et al. (33). Nanopore reads were obtained using a genomic DNA library prepared in accordance with the Nanopore 1D ligation protocol, using MinION SPOT ON MK1 R9 flow cells and the raw data were converted to sequence data via MinKnow

FIG 3 Legend (Continued)
(C) Chromatogram from the empty vector (pESAC-13A) control strain *S. coelicolor* M1152, indicating the absence of an aurodox-associated peak. (D) Chromatogram of extract from the growth of *S. coelicolor* M1152/pAur1. The aurodox peak is visible at 7.12 min, and the MS data indicate the presence of aurodox. (E) Chromatogram of extracts from *S. coelicolor* M1152/pAur1Δ*aurA*1 showing absence of an aurodox-associated peak. Corresponding MS data can be found in Fig. S4. (F) Bioactivity of the extracts used in A to E, indicating the zones of inhibition associated with the extracts by disc diffusion against *Staphylococcus aureus* ATCC 43300.

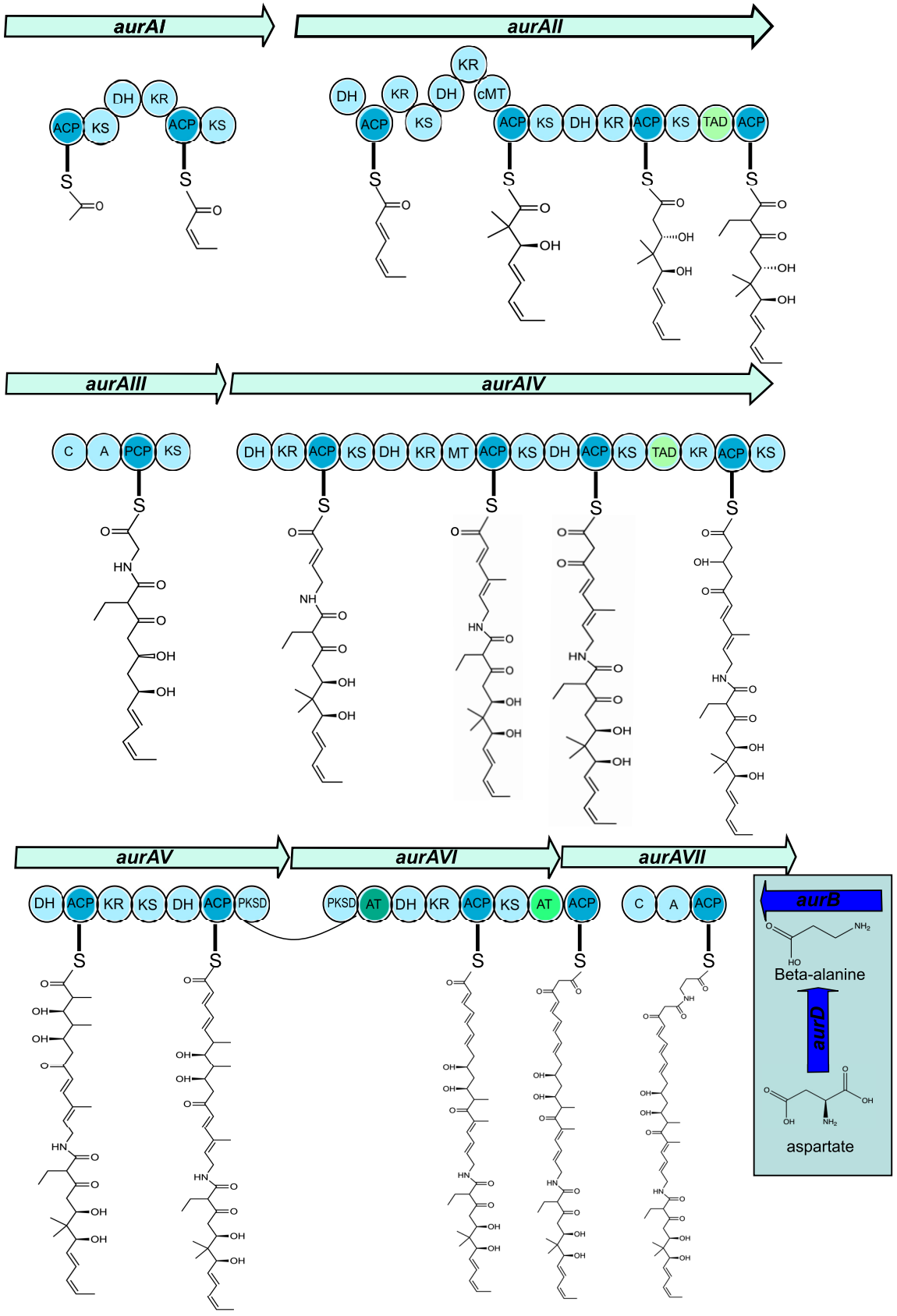

FIG 4 Summary of the enzymatic reactions carried out by AurAI-AurAVII In aurodox PKS backbone biosynthesis. ACP: acyl carrier protein; AT: acyltransferase domain; C: condensation domain; DH: dehydratase domain ER: enoyl reductase domain; KR: keto reductase domain; KS: keto synthase domain; MT: methyl transferase domain; PCP: peptidyl carrier protein; TAD: trans-AT docking domain.

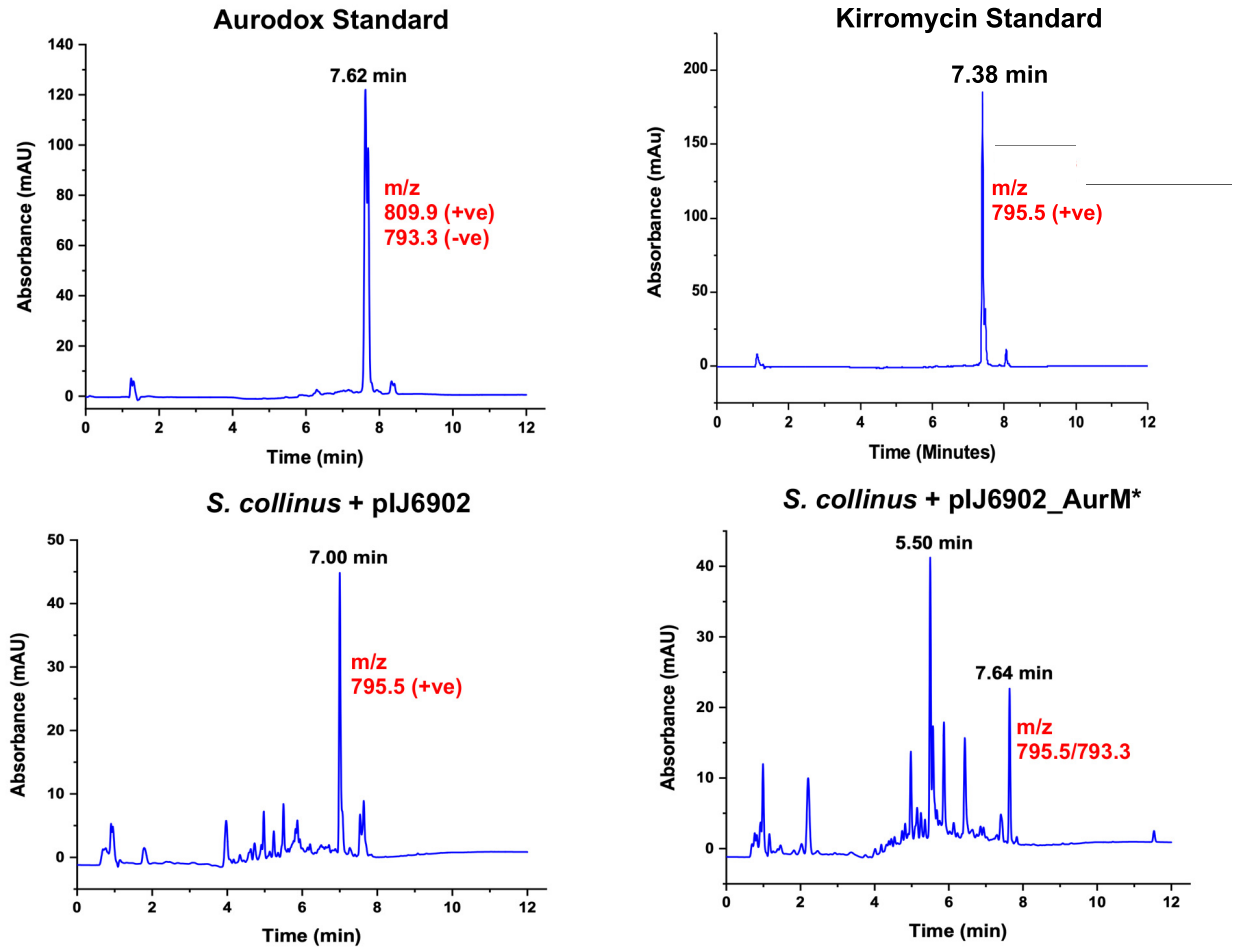

FIG 5 Methylation of kirromycin is the last step in aurodox biosynthesis and is catalyzed by AurM*. Chromatograms of aurodox and kirromycin standards and fermentation extracts from a control strain *S. collinus* Tü 365 containing pIJ6902 (empty vector control) show the presence of kirromycin and absence of aurodox-associated mass and chromatograms from extracts from *S. collinus* Tü 365 containing pIJ6902_AurM*. Corresponding MS data can be found in Fig. S5.

base-calling software. Illumina data were obtained from Microbes NG (Birmingham, UK) using the HiSeq 2500 sequencing platform. Reads were adapter trimmed using Trimmomatic 0.30 (34) with a sliding window quality cutoff Q15. PacBio sequencing was provided by Nu-omics at (the University of Northumbria, UK) using the PacBio Sequel instrument, and contigs were assembled in HGAP4.

Streptomyces goldiniensis genome was assembled using SPAdes (34) using data provided by all three platforms. AutoMLST (35) was used to determine the closest neighbor *S. bottropensis* ATCC 25435, Taxonomy ID: 1054862) which was used for scaffold-based assembly via MeDuSa (36) with the quality analysis carried out using QUAST (37). Annotation of the *Streptomyces goldiniensis* genome was created using Prokka (38) and can be accessed at the GenBank Bioproject PRJNA602141. Biosynthetic gene cluster identification was carried out using antiSMASH bacterial version 5.0.0 with modular enzymatic domains analysis carried out using the PKS/NRPS domain annotation function in antiSMASH (18).

Aurodox production, purification, and detection. *Streptomyces* spore stocks (1×10^8 spores) were pregerminated in 10 mL of GYM medium (32) overnight at 30°C with shaking at 250 rpm. Cells were then washed three times to remove antibiotics (if used) and resuspended in 1 mL of GYM, which was used to inoculate a 50 mL seed culture of GYM which was incubated at 30°C with shaking at 250 rpm. After 7 days, biomass was removed by centrifugation (4000 $\times$ *g*, 10 min) and culture supernatant was filter sterilized through a 0.2 μM Millipore filter. Supernatants were mixed with an equal volume of chloroform and a separation funnel was used to remove the lower, solvent phase. Solvent extracts were dried under nitrogen and extracts were solubilized in ethanol for LC-MS analysis. Authentic aurodox standard (1 mg/mL) was purchased from Enzo (New York, USA). LC-MS was carried out on an Agilent 1100 HPLC instrument in conjunction with a Waters Micromass ZQ 2000/4000 mass detector. Electrospray ionization (ESI) was used in all cases. The RP-HPLC analysis was conducted on a Zorbax 45 mm x 150 mm C18 column at 40°C. Ammonium acetate buffers were used as follows: Buffer A (5 mM Ammonium acetate in Water) and Buffer B (5 mM Ammonium acetate in acetonitrile). Positive and negative electrospray

methods were applied with 100 to 1000 AMU positive, and 120 to 1000 AMU negative with a scanning time of 0.5 s. The UV detection was carried out at 254 nm.

Construction of aurodox expression strains and deletion mutant. Aurodox encoding vector pAur1 (Bio S & T, Canada) and empty vector pESAC-13A (39) were transferred to the nonmethylating *Escherichia coli* strain ET12567 via tri-parental mating. Briefly, fresh overnight cultures of *E. coli* DH10β containing pAur1 or the parental vector pESAC-13A (apramycin resistant), *E. coli* Top10 containing the driver plasmid pR9604 (Beta-lactam resistant), and ET12567 (Chloramphenicol resistant) were to an optical density at 600 nm (OD_{600}) of 0.6. Cells were washed three times in fresh LB by centrifugation at 4000 $\times$ *g* and resuspended in 1 mL of LB. A 20 μL aliquot of each strain was plated in the center of an LB plate and incubated at 37°C overnight. The resulting growth was restreaked on to the required antibiotic selection and the presence of the conjugating vector in the *E. coli* ET12567/pR9604 strain was confirmed via colony PCR. Mutation in pAur1 was carried out according to the ReDirect PCR targeting system in *Streptomyces* (21), using the hygromycin resistance cassette, pIJ10700 as the disruption cassette (http://streptomyces.org.uk/redirect/RecombineeringFEMSMP-2006-5.pdf). Disrupted PACs were introduced into *E. coli* ET12567/pR9604 via tri-parental mating and subsequently moved into *Streptomyces coelicolor* M1152 via conjugation as described above.

Cloning of *aurM from *Streptomyces goldiniensis*.** The putative *O*-methyltransferase *aurM** was amplified from *S. goldiniensis* genomic DNA using the oligonucleotide primers in Table S5 (https://doi.org/10.6084/m9.figshare.19140005.v1) and cloned using the NEB Gibson Assembly cloning kit into pIJ6902 (24). Conjugation of pIJ6902-based vectors was according to Kieser et al. (33).

Bioassays. Bioassays were conducted using disc diffusion assays with *Streptomyces* fermentation extracts on soft nutrient overlays containing *Staphylococcus aureus* ATCC 43300 as the indicator organism.

Data availability. Genome sequence data for *Streptomyces goldiniensis* is available at GenBank Bioproject PRJNA602141. All other supplementary data and supporting figures are publicly available at https://doi.org/10.6084/m9.figshare.19140005.v1.

ACKNOWLEDGMENTS

We thank Wolfgang Wohlleben (University of Tübingen) for the gift of the *Streptomyces collinus* Tü 365 strain, Margherita Sosio (Naicons) for the gift of pESAC-13A. and Mervyn Bibb (John Innes Centre) for the gift of the *S. coelicolor* M1152 strain. We also thank Iain S. Hunter (University of Strathclyde) and Matt Hutchings (John Innes Centre) for helpful discussions.

We thank the University of Strathclyde and the University of Glasgow for jointly funding the Ph.D. of REM. A.J.R., and P.A.H. would like to acknowledge funding from Medical Research Council (MRC) (MR/V011499/1). P.A.H. would also like to acknowledge funding from Biotechnology and Biological Sciences Research Council (BBSRC) (BB/T001038/1 and BB/T004126/1) and the Royal Academy of Engineering Research Chair Scheme for long-term personal research support (RCSRF2021\11\15).

The funders had no role in study design, data collection, interpretation, or the decision to submit the work for publication.

We declare no conflict of interest.

REFERENCES

1. Chevrette MG, Gutiérrez-García K, Selem-Mojica N, Aguilar-Martínez C, Yañez-Olvera A, Ramos-Aboites HE, Hoskisson PA, Barona-Gómez F. 2019. Evolutionary dynamics of natural product biosynthesis in bacteria. Nat Prod Rep 37:566–599. https://doi.org/10.1039/c9np00048h.
2. Berger J, Lehr HH, Teitel S, Maehr H, Grunberg E. 1973. A new antibiotic X-5108 of *Streptomyces* origin. J Antibiot (Tokyo) 26:15–22. https://doi.org/10.7164/antibiotics.26.15.
3. Vogeley L, Palm GJ, Mesters JR, Hilgenfeld R. 2001. Conformational change of elongation factor Tu (EF-Tu) induced by antibiotic binding crystal structure of the complex between EF-Tu·GDP and aurodox. J Biol Chem 276:17149–17155. https://doi.org/10.1074/jbc.M100017200.
4. Prezioso SM, Brown NE, Goldberg JB. 2017. Elfamycins: inhibitors of elongation factor-Tu. Mol Microbiol 106:22–34. https://doi.org/10.1111/mmi.13750.
5. Kimura K, Iwatsuki M, Nagai T, Matsumoto A, Takahashi Y, Shiomi K, Omura S, Abe A. 2011. A small-molecule inhibitor of the bacterial type III secretion system protects against in vivo infection with *Citrobacter rodentium*. J Antibiot (Tokyo) 64:197–203. https://doi.org/10.1038/ja.2010.155.
6. McHugh RE, O'Boyle N, Connolly JPR, Hoskisson PA, Roe AJ. 2018. Characterization of the mode of action of aurodox, a type III secretion system inhibitor from *Streptomyces goldiniensis*. Infect Immun 87:e00595-18.
7. Weber T, Laiple KJ, Pross EK, Textor A, Grond S, Welzel K, Pelzer S, Vente A, Wohlleben W. 2008. Molecular analysis of the kirromycin biosynthetic gene cluster revealed β-alanine as precursor of the pyridone moiety. Chemistry & Biology 15:175–188. https://doi.org/10.1016/j.chembiol.2007.12.009.
8. Robertsen HL, Musiol-Kroll EM, Ding L, Laiple KJ, Hofeditz T, Wohlleben W, Lee SY, Grond S, Weber T. 2018. Filling the gaps in the kirromycin biosynthesis: deciphering the role of genes involved in ethylmalonyl-CoA supply and tailoring reactions. Sci Rep 8:3230. https://doi.org/10.1038/s41598-018-21507-6.
9. Laiple KJ, Härtner T, Fiedler H-P, Wohlleben W, Weber T. 2009. The kirromycin gene cluster of *Streptomyces collinus* Tü 365 codes for an aspartate-α-decarboxylase, KirD, which is involved in the biosynthesis of the precursor β-alanine. J Antibiot (Tokyo) 62:465–468. https://doi.org/10.1038/ja.2009.67.
10. Pavlidou M, Pross EK, Musiol EM, Kulik A, Wohlleben W, Weber T. 2011. The phosphopantetheinyl transferase KirP activates the ACP and PCP domains of the kirromycin NRPS/PKS of Streptomyces collinus Tü 365. FEMS Microbiol Lett 319:26–33. https://doi.org/10.1111/j.1574-6968.2011.02263.x.
11. Deng W, Puente JL, Gruenheid S, Li Y, Vallance BA, Vázquez A, Barba J, Ibarra JA, O'Donnell P, Metalnikov P, Ashman K, Lee S, Goode D, Pawson T, Finlay BB. 2004. Dissecting virulence: systematic and functional analyses of a pathogenicity island. Proc Natl Acad Sci U S A 101:3597–3602. https://doi.org/10.1073/pnas.0400326101.
12. Goldwater PN, Bettelheim KA. 2012. Treatment of enterohemorrhagic *Escherichia coli* (EHEC) infection and hemolytic uremic syndrome (HUS). BMC Med 10:12. https://doi.org/10.1186/1741-7015-10-12.

13. Huerta-Uribe A, Marjenberg ZR, Yamaguchi N, Fitzgerald S, Connolly JPR, Carpena N, Uvell H, Douce G, Elofsson M, Byron O, Marquez R, Gally DL, Roe AJ. 2016. Identification and characterization of novel compounds blocking shiga toxin expression in *Escherichia coli* O157:H7. Front Microbiol 7:1930.
14. Melton-Celsa AR. 2014. Shiga toxin (Stx) classification, structure, and function. Microbiol Spectr 2:EHEC. https://doi.org/10.1128/microbiolspec.EHEC-0024-2013.
15. Nguyen Y, Sperandio V. 2012. Enterohemorrhagic *E. coli* (EHEC) pathogenesis. Front Cell Infect Microbiol 2:90. https://doi.org/10.3389/fcimb.2012.00090.
16. Fuchs S, Mühldorfer I, Donohue-Rolfe A, Kerényi M, Emödy L, Alexiev R, Nenkov P, Hacker J. 1999. Influence of RecA onin vivovirulence and Shiga toxin 2 production in *Escherichia coli* pathogens. Microb Pathog 27:13–23. https://doi.org/10.1006/mpat.1999.0279.
17. McHugh RE, Munnoch JT, Roe AJ, Hoskisson PA. 2021. Genome sequence of the aurodox-producing bacterium *Streptomyces goldiniensis* ATCC 21386. Access Microbiol 4. https://doi.org/10.1099/acmi.0.000358.
18. Blin K, Shaw S, Steinke K, Villebro R, Ziemert N, Lee SY, Medema MH, Weber T. 2019. antiSMASH 5.0: updates to the secondary metabolite genome mining pipeline. Nucleic Acids Res 47:W81–W87. https://doi.org/10.1093/nar/gkz310.
19. Sosio M, Giusino F, Cappellano C, Bossi E, Puglia AM, Donadio S. 2000. Artificial chromosomes for antibiotic-producing actinomycetes. Nat Biotechnol 18:343–345. https://doi.org/10.1038/73810.
20. Paget MS, Chamberlin L, Atrih A, Foster SJ, Buttner MJ. 1999. Evidence that the extracytoplasmic function sigma factor sigmaE is required for normal cell wall structure in *Streptomyces coelicolor* A3(2). J Bacteriol 181:204–211. https://doi.org/10.1128/JB.181.1.204-211.1999.
21. Gust B, Challis GL, Fowler K, Kieser T, Chater KF. 2003. PCR-targeted *Streptomyces* gene replacement identifies a protein domain needed for biosynthesis of the sesquiterpene soil odor geosmin. Proc Natl Acad Sci U S A 100:1541–1546. https://doi.org/10.1073/pnas.0337542100.
22. de los Santos EL, Challis G. 2019. clusterTools: functional element identification for the in silico prioritization of biosynthetic gene clusters. Access Microbiol 1:301. https://doi.org/10.1099/acmi.ac2019.po0154.
23. Rausch C, Weber T, Kohlbacher O, Wohlleben W, Huson DH. 2005. Specificity prediction of adenylation domains in nonribosomal peptide synthetases (NRPS) using transductive support vector machines (TSVMs). Nucleic Acids Res 33:5799–5808. https://doi.org/10.1093/nar/gki885.
24. Huang J, Shi J, Molle V, Sohlberg B, Weaver D, Bibb MJ, Karoonuthaisiri N, Lih C, Kao CM, Buttner MJ, Cohen SN. 2005. Cross-regulation among disparate antibiotic biosynthetic pathways of *Streptomyces coelicolor*. Mol Microbiol 58:1276–1287. https://doi.org/10.1111/j.1365-2958.2005.04879.x.
25. Jensen PR. 2016. Natural products and the gene cluster revolution. Trends Microbiol 24:968–977. https://doi.org/10.1016/j.tim.2016.07.006.
26. Kim SY, Ju K-S, Metcalf WW, Evans BS, Kuzuyama T, van der Donk WA. 2012. Different biosynthetic pathways to fosfomycin in *Pseudomonas syringae* and *Streptomyces* species. Antimicrob Agents Chemother 56:4175–4183. https://doi.org/10.1128/AAC.06478-11.
27. Sit CS, Ruzzini AC, Arnam EBV, Ramadhar TR, Currie CR, Clardy J. 2015. Variable genetic architectures produce virtually identical molecules in bacterial symbionts of fungus-growing ants. Proc Natl Acad Sci U S A 112:13150–13154. https://doi.org/10.1073/pnas.1515348112.
28. Grenade NL, Howe GW, Ross AC. 2021. The convergence of bacterial natural products from evolutionarily distinct pathways. Curr Opin Biotechnol 69:17–25. https://doi.org/10.1016/j.copbio.2020.10.009.
29. Beld J, Sonnenschein EC, Vickery CR, Noel JP, Burkart MD. 2014. The phosphopantetheinyl transferases: catalysis of a post-translational modification crucial for life. Nat Prod Rep 31:61–108. https://doi.org/10.1039/c3np70054b.
30. Gui C, Li Q, Mo X, Qin X, Ma J, Ju J. 2015. Discovery of a new family of dieckmann cyclases essential to tetramic acid and pyridone-based natural products biosynthesis. Org Lett 17:628–631. https://doi.org/10.1021/ol5036497.
31. McKean IJW, Hoskisson PA, Burley GA. 2020. Biocatalytic alkylation cascades: recent advances and future opportunities for late-stage functionalization. Chembiochem 21:2890–2897. https://doi.org/10.1002/cbic.202000187.
32. McKean IJW, Sadler JC, Cuetos A, Frese A, Humphreys LD, Grogan G, Hoskisson PA, Burley GA. 2019. S-adenosyl methionine cofactor modifications enhance the biocatalytic repertoire of small molecule C-alkylation. Angew Chem Int Ed Engl 58:17583–17588. https://doi.org/10.1002/anie.201908681.
33. Kieser T, Bibb M, Buttner M, Chater K, Hopwood DA. 2000. Practical Streptomyces Genetics. John Innes Foundation.
34. Bankevich A, Nurk S, Antipov D, Gurevich AA, Dvorkin M, Kulikov AS, Lesin VM, Nikolenko SI, Pham S, Prjibelski AD, Pyshkin AV, Sirotkin AV, Vyahhi N, Tesler G, Alekseyev MA, Pevzner PA. 2012. SPAdes: a new genome assembly algorithm and its applications to single-cell sequencing. J Comput Biol 19:455–477. https://doi.org/10.1089/cmb.2012.0021.
35. Alanjary M, Steinke K, Ziemert N. 2019. AutoMLST: an automated web server for generating multi-locus species trees highlighting natural product potential. Nucleic Acids Res 47:W276–W282. https://doi.org/10.1093/nar/gkz282.
36. Bosi E, Donati B, Galardini M, Brunetti S, Sagot M-F, Lió P, Crescenzi P, Fani R, Fondi M. 2015. MeDuSa: a multi-draft based scaffolder. Bioinformatics 31:2443–2451. https://doi.org/10.1093/bioinformatics/btv171.
37. Gurevich A, Saveliev V, Vyahhi N, Tesler G. 2013. QUAST: quality assessment tool for genome assemblies. Bioinformatics 29:1072–1075. https://doi.org/10.1093/bioinformatics/btt086.
38. Seemann T. 2014. Prokka: rapid prokaryotic genome annotation. Bioinformatics 30:2068–2069. https://doi.org/10.1093/bioinformatics/btu153.
39. Sosio M, Bossi E, Donadio S. 2001. Assembly of large genomic segments in artificial chromosomes by homologous recombination in *Escherichia coli*. Nucleic Acids Res 29:e37. https://doi.org/10.1093/nar/29.7.e37.